

Molecular Cell, Volume 74

Supplemental Information

TAF5L and TAF6L Maintain Self-Renewal of Embryonic

Stem Cells via the MYC Regulatory Network

Davide Seruggia, Martin Oti, Pratibha Tripathi, Matthew C. Canver, Lucy LeBlanc, Dafne C. Di Giammartino, Michael J. Bullen, Christian M. Nefzger, Yu Bo Yang Sun, Rick Farouni, Jose M. Polo, Luca Pinello, Effie Apostolou, Jonghwan Kim, Stuart H. Orkin, and Partha Pratim Das

SUPPLEMENTAL INFORMATION

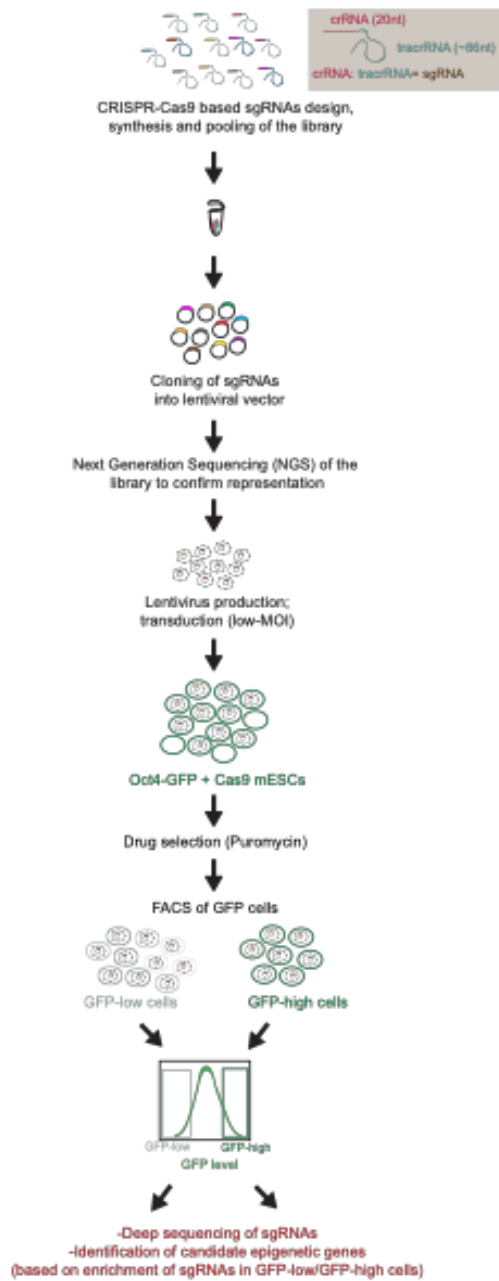
TAF5L and TAF6L maintain self-renewal of embryonic stem cells via the MYC regulatory network

Davide Seruggia, Martin Oti, Pratibha Tripathi, Matthew C. Canver, Lucy LeBlanc, Dafne C. Di Giammartino, Michael J. Bullen, Christian M. Nefzger, Yu Bo Yang Sun, Rick Farouni, Jose M. Polo, Luca Pinello, Effie Apostolou, Jonghwan Kim, Stuart H. Orkin and Partha Pratim Das

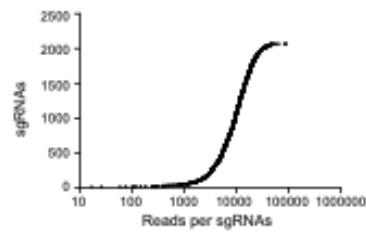
SUPPLEMENTAL FIGURES, TITLES AND LEGENDS

Figure S1

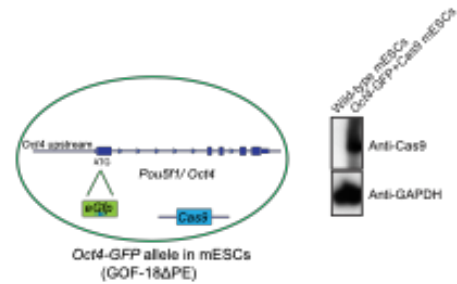
A



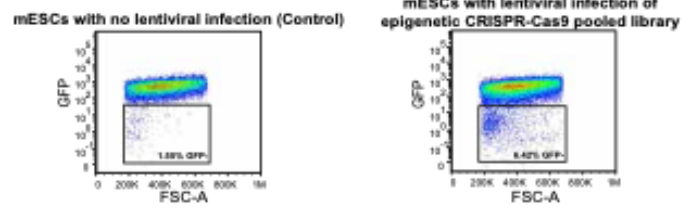
B



C



D



E

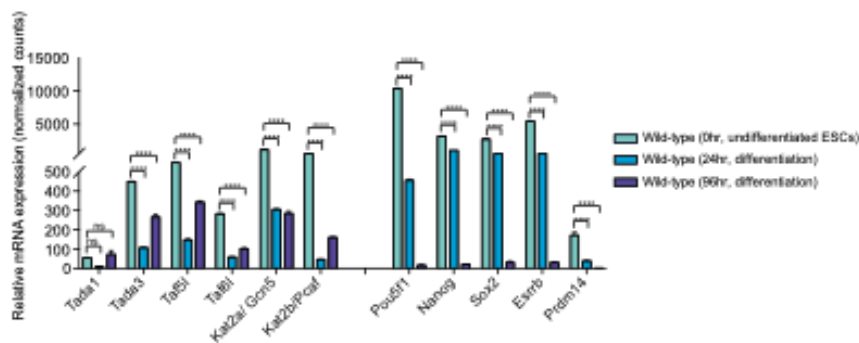


Figure S1. CRISPR-Cas9 mediated loss-of-function genetic screen identifies potential candidate epigenetic genes for the mESC state

(A) Schematic diagram represents an outline of the CRISPR-Cas9 screen.

(B) Representation of the epigenetic CRISPR-Cas9 pooled library. The pooled library comprised of 2,335 sgRNAs was synthesized and cloned into a lentiviral vector, and deep-sequenced to ensure representation of the sgRNAs. Each dot represents an sgRNA and its corresponding read count in the pooled library. Y axis: sgRNAs; X axis: number of reads per sgRNAs.

(C) *Oct4*-GFP reporter mESC line (Yeom et al., 1996 and Szabo et al., 2002) that constitutively expresses Cas9. Cas9 expression was confirmed by Western blot.

(D) FACS analysis represents percentage (%) of GFP-ve (GFP-low) cells from *Oct4*-GFP reporter mESCs either with no lentiviral infection (control) or with lentiviral infection of epigenetic CRISPR-Cas9 pooled library at low multiplicity (MOI).

(E) mRNA expression levels of selected candidate epigenetic genes (*Taf5l*, *Taf6l*, *Tada1* and *Tada3*), ESC specific genes (*Pou5f1/Oct4*, *Nanog*, *Sox2*, *Esrrb*, *Prdm14*), and HAT complex genes (*Kat2a* and *Kat2b*) during differentiation – from undifferentiated ESCs to differentiated state (0 to 24 to 96 hrs).

Data are represented as mean \pm SEM (n = 3); p-values were calculated using ANOVA.

*p < 0.05; **p < 0.01; ***p < 0.001; ****p < 0.0001; and ns (non-significant).

Related to Figure 1.

Figure S2

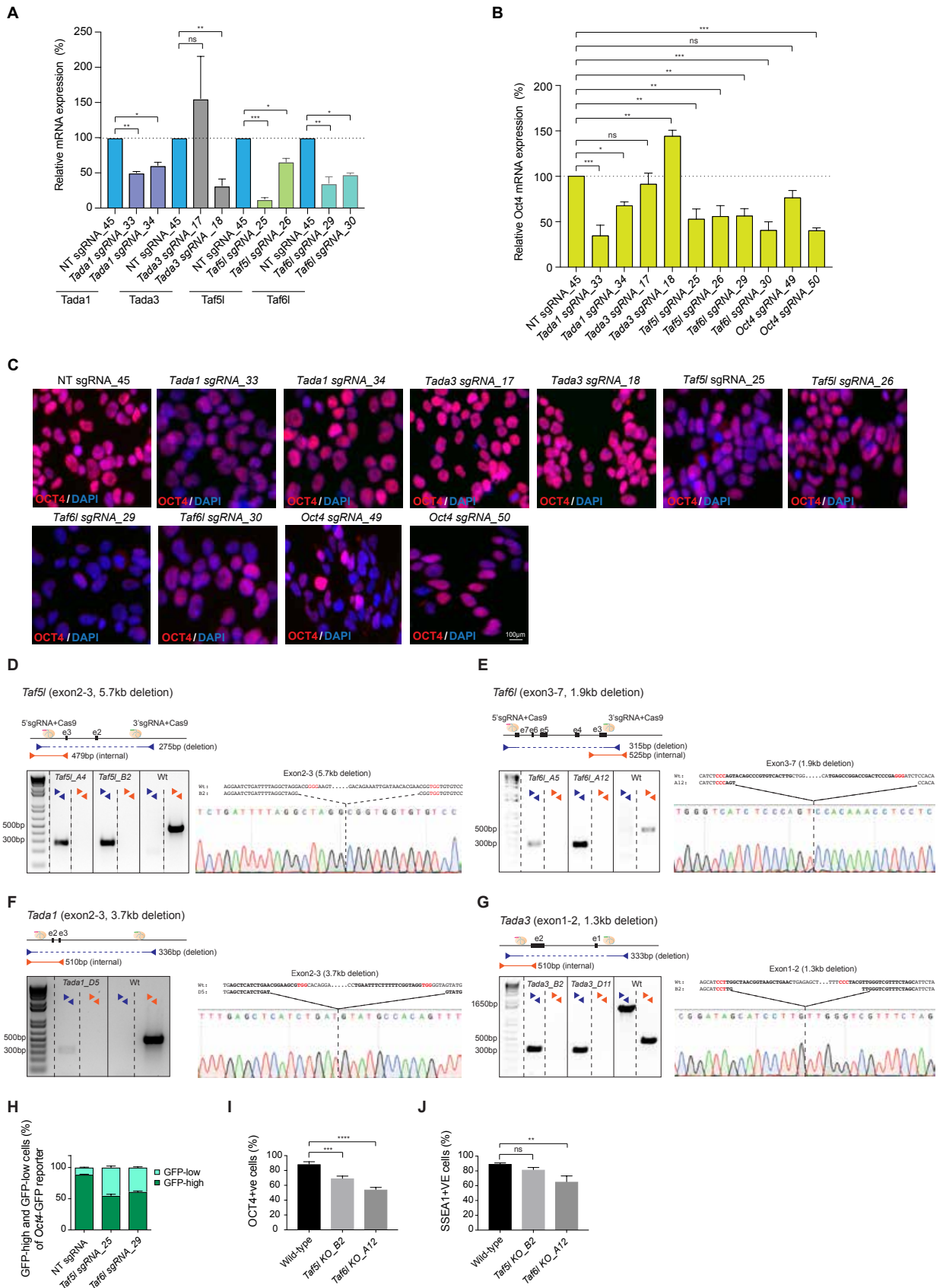


Figure S2. Validation confirms TAF5L and TAF6L are the epigenetic genes for the mESC state

(A) mRNA expression levels of *Tada1*, *Tada3*, *Taf5l* and *Taf6l* after delivery of individual sgRNAs that target coding sequences of these genes and create indels. Non-targeting sgRNA (NT sgRNA) used as control. mRNA levels were normalized to GAPDH. The two best sgRNAs (for each gene) from the screen were used.

(B) Endogenous *Oct4* mRNA expression levels in the *Tada1*, *Tada3*, *Taf5l* and *Taf6l* edited cells.

(C) Immunofluorescence staining of OCT4 in the *Tada1*, *Tada3*, *Taf5l* and *Taf6l* edited cells. Scale bar is 100 μ m.

(D-G) Schematic diagram illustrating the strategy to generate homozygous/biallelic deletion or *KO* clones. Paired sgRNAs (5' and 3' sgRNAs) flanking critical exons of *Taf5l* (D), *Taf6l* (E), *Tada1* (F) and *Tada3* (G) were introduced to create homozygous deletions. Two PCRs (deletion PCR and internal PCR) were used for each targeted gene to identify biallelic/homozygous deletions. Sanger sequencing was used to confirm the biallelic deletions. The *KO* clones show the same deletion breakpoints in both alleles.

(H) Percentages of GFP-high and GFP-low cells of *Oct4*-GFP reporter mESCs upon delivery of non-targeting (NT) or *Taf5l* and *Taf6l* targeting sgRNAs.

(I-J) Percentages of OCT4-positive (I) and SSEA1-positive (J) cells in wild-type, *Taf5l KO* and *Taf6l KO* mESCs.

Data are represented as mean \pm SEM (n = 3); p-values were calculated using ANOVA.

*p < 0.05; **p < 0.01; ***p < 0.001; ****p < 0.0001; and ns (non-significant).

Related to Figure 2.

Figure S3

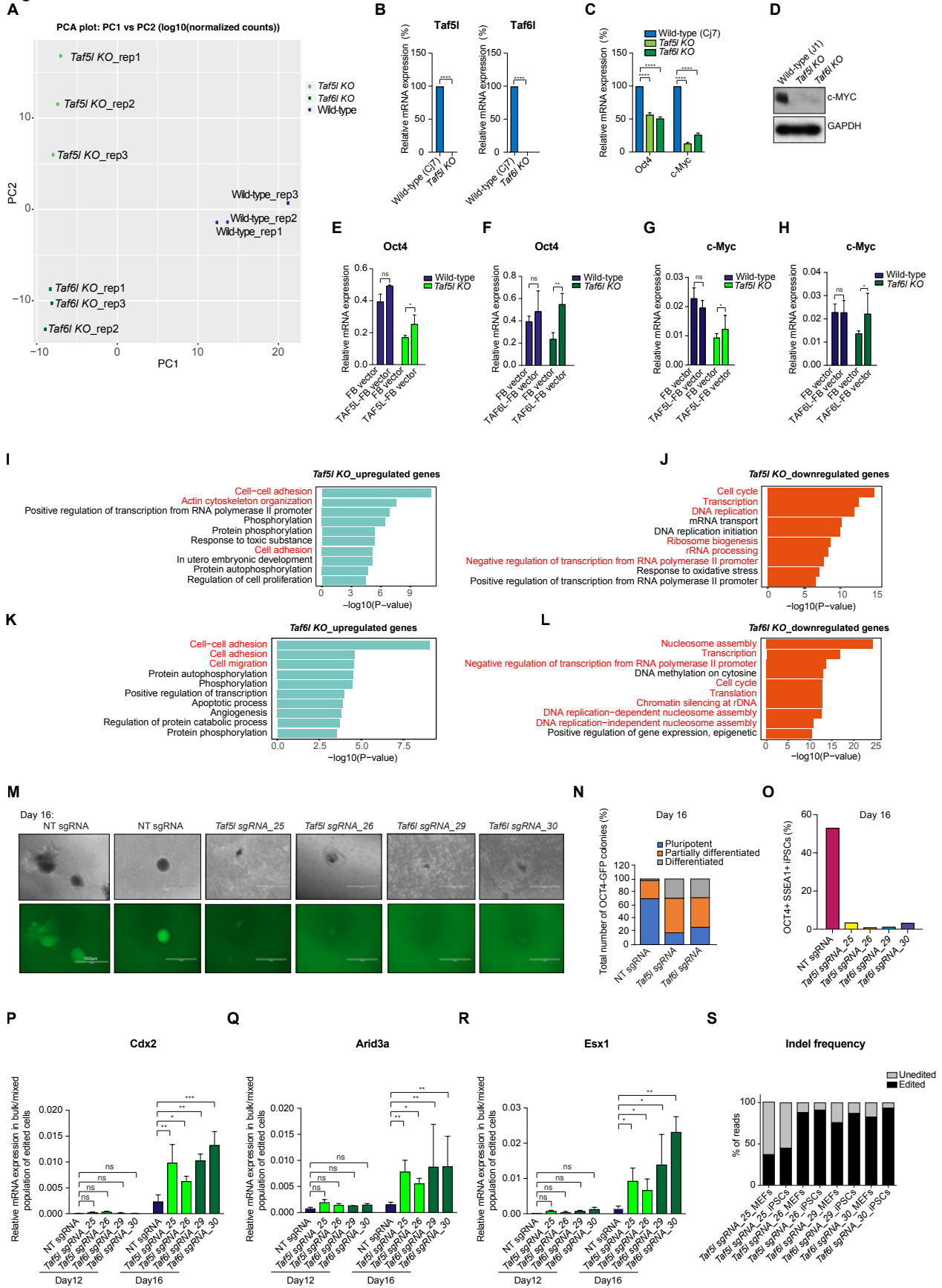


Figure S3. TAF5L and TAF6L are required for gene expression programs of mESC state; and for somatic cell reprogramming/iPSCs generation

(A) PCA plot of RNAseq data from three biological replicates of wild-type, *Taf5l* KO and *Taf6l* KO.

(B) mRNA expression levels of *Taf5l* and *Taf6l* in wild-type (CJ7) and their corresponding KOs.

(C) mRNA expression levels of Oct4 and c-Myc from wild-type (CJ7), *Taf5l* KO and *Taf6l* KO (from RT-qPCR).

(D) Protein levels of c-MYC in wild-type (J1) and KOs, using Western blot.

(E, F) Oct4 mRNA expression levels upon exogenous expression of TAF5L and TAF6L in their corresponding KOs and wild-type.

(G, H) c-Myc mRNA expression levels upon exogenous expression of TAF5L and TAF6L in their corresponding KOs and wild-type.

(I-L) Gene ontology (GO) term analysis (biological process) of up and downregulated genes from *Taf5l* and *Taf6l* KOs.

(M) Morphology and GFP fluorescence of transgene-independent iPSC colonies (at day 16 after reprogramming) that were generated upon perturbation of *Taf5l* and *Taf6l* using sgRNAs. Non-targeting sgRNA used as a control. Scale bar is 1000 μ m.

(N) Percentages of pluripotent iPSCs, partially differentiated and differentiated cells after reprogramming (at day 16) upon perturbation of *Taf5l* and *Taf6l* using sgRNAs. Non-targeting sgRNA used as a control.

(O) FACS analysis of OCT4+ and SSEA1+ iPSCs at day 16.

(P-R) mRNA expression levels of *Cdx2*, *Arid3a* and *Esx1* in bulk/mixed populations of edited cells after reprogramming at day 12 and day 16, upon perturbation of *Taf5l* and *Taf6l* using sgRNAs. Non-targeting sgRNA used as control.

(S) Percentages of indels (insertions and deletions) of the targeted regions of *Taf5l* and *Taf6l* genes were quantified using targeted amplicon sequencing. Indel frequencies of *Taf5l* and *Taf6l* genes were measured before (from mCherry+ reprogrammable MEFs, as MEFs were transduced with viral particles of sgRNAs carrying mCherry and Cas9) and after (bulk/mixed populations of edited cells) reprogramming at day 16. Percentages indicate the edited reads over the total number of reads.

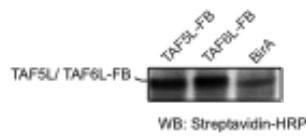
Data are represented as mean \pm SEM (n = 3); p-values were calculated using ANOVA.

*p < 0.05; **p < 0.01; ***p < 0.001; ****p < 0.0001; and ns (non-significant).

Related to Figure 3.

Figure S4

A



B

TAF5L interacting partners identified by MS (150mM salt)

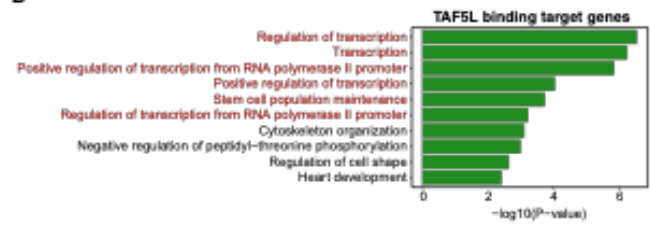
Interacting partners		TAF5L-FB (no. of peptides)	BirA (no. of peptides)
Trrap	HAT	30	0
Taf6l	HAT	16	0
Taf5l	HAT	16	0
Taf9	HAT	14	0
Supt20h	HAT	11	0
Taf9b	HAT	10	0
Tada1	HAT	9	0
Tada3	HAT	8	0
Supt7l	HAT	8	0
Flna		6	0
Hmnhp1		4	0
L11d1		3	0
Supt3	HAT	3	0
Sf3b3		3	0
Sgt29		3	0
Kat2b	HAT	3	0
Abn713		3	0
Taf10	HAT	3	0
Cpne8		3	0

C

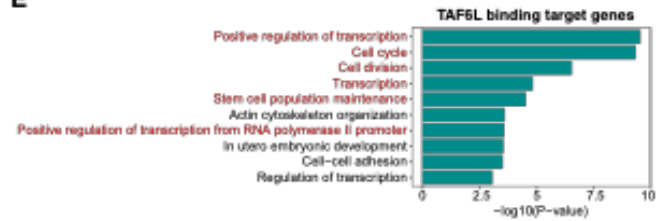
TAF6L interacting partners identified by MS (150mM salt)

Interacting partners		TAF6L-FB (no. of peptides)	BirA (no. of peptides)
Trrap	HAT	77	0
Taf6l	HAT	47	0
Taf5l	HAT	39	0
Supt7l	HAT	22	0
Supt20h	HAT	20	0
Taf9	HAT	17	0
Tada3	HAT	16	0
Taf9b	HAT	14	0
Sf3b3		12	0
Kat2b	HAT	11	0
Tdh		11	0
Supt3	HAT	11	0
Tada1	HAT	9	0
Taf10	HAT	9	0
Hadha		7	0
Atp5b		6	0
Kat2a	HAT	6	0
Tada2b	HAT	6	0
Abn712		5	0
Hsp90ab1		5	0
Lomp1		4	0
Sgt29		4	0
Supt20	HAT	5	0
Trap1		3	0
Pdha1		3	0
Atad3		3	0
Pdxb		3	0
Hmnhp1		3	0
Ywhaz		3	0

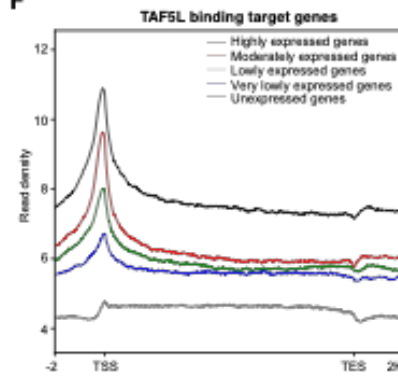
D



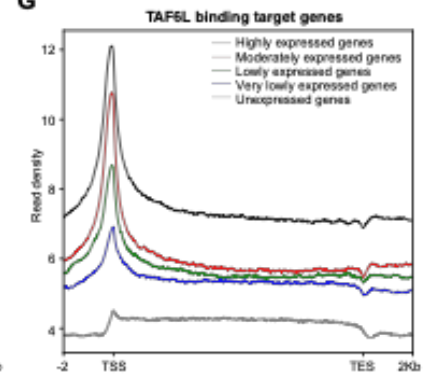
E



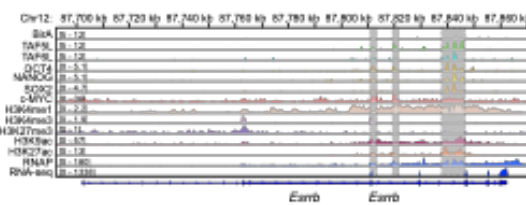
F



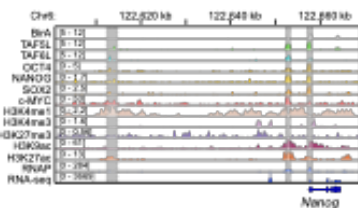
G



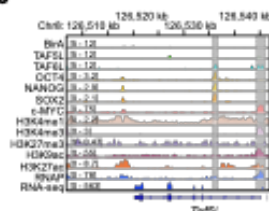
H



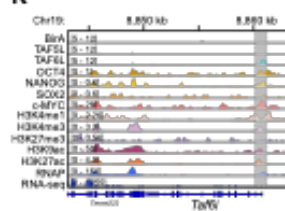
I



J



K



L

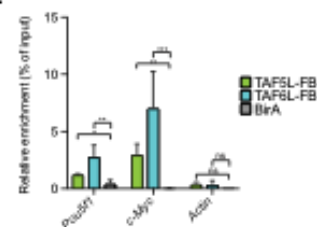


Figure S4. TAF5L and TAF6L belong to the MYC and CORE regulatory modules but mainly regulate the MYC module activity

(A) Generation of flag-biotin (FB)-tagged TAF5L and TAF6L mESC lines. The biotinylated forms of TAF5L and TAF6L were detected using streptavidin.

(B, C) Interacting partners of TAF5L and TAF6L are displayed. These interacting partners were identified through pull down of the biotinylated version of TAF5L and TAF6L using streptavidin beads, followed by mass spectrometry.

(D, E) Gene ontology (GO) term analysis (biological processes) of TAF5L and TAF6L binding target genes.

(F, G) Distribution of TAF5L and TAF6L binding target genes around the five different metagenes— ranked by their expression levels in mESCs.

(H-K) Genomic tracks of ChIP intensities of several factors, including TAF5L and TAF6L, and histone marks binding at *Esrrb*, *Nanog*, *Taf5l* and *Taf6l* gene loci. RNAseq tracks represent expression of these genes.

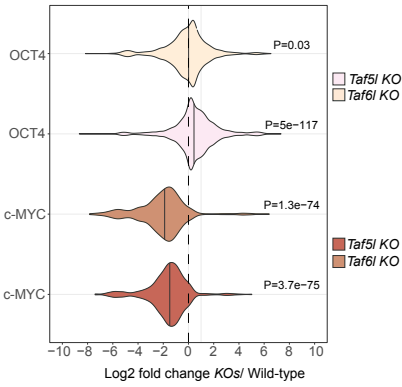
(L) ChIP-qPCR analyses of TAF5L and TAF6L binding at *Oct4*, *c-Myc* and *Actin* gene loci. Relative enrichment is shown as % of input (all the factors multiplied with 10^6).

Related to Figure 4.

Figure S5

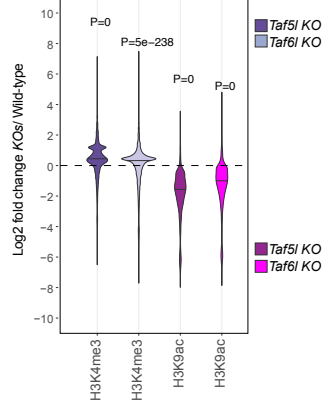
A

Global differential binding of OCT4 and c-MYC in *Taf5l* & *Taf6l* KOs compared to Wild-type



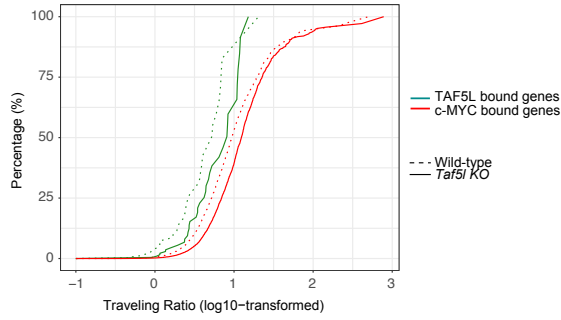
B

Global differential binding of H3K4me3 and H3K9ac in *Taf5l* & *Taf6l* KOs compared to Wild-type



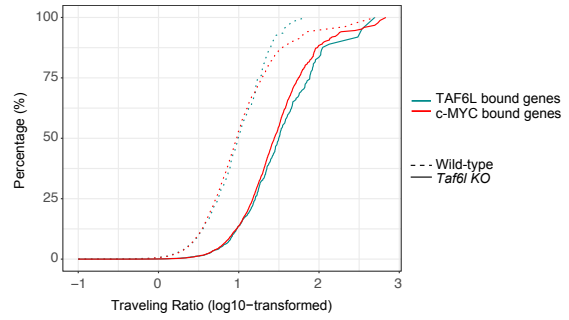
C

Traveling Ratio of RNA Pol II-Ser 2p at c-MYC and TAF5L bound genes in *Taf5l* KO and Wild-type



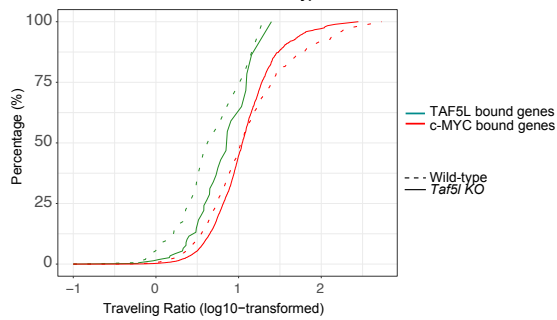
D

Traveling Ratio of RNA Pol II-Ser 2p at c-MYC and TAF6L bound genes in *Taf6l* KO and Wild-type



E

Traveling Ratio of RNA Pol II-Ser 5p at c-MYC and TAF5L bound genes in *Taf5l* KO and Wild-type



F

Traveling Ratio of RNA Pol II-Ser 5p at c-MYC and TAF6L bound genes in *Taf6l* KO and Wild-type

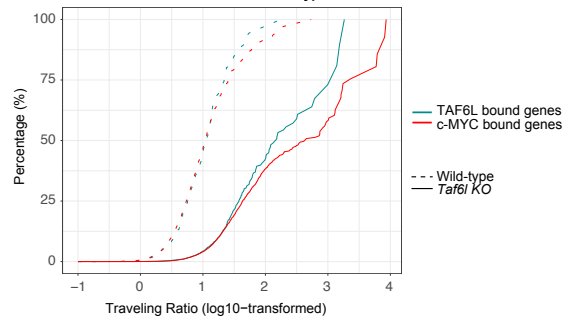


Figure S5. Predominantly TAF5L/TAF6L modulate H3K9ac deposition and c-MYC recruitment at the TAF5L/TAF6L target genes to activate their gene expression through RNA Pol II pause release

(A) Global differential binding of OCT4 and c-MYC in *Taf5l* and *Taf6l* KOs compared to wild-type.

(B) Global differential binding of H3K9ac and H3K4me3 in *Taf5l* and *Taf6l* KOs compared to wild-type.

(C) The traveling ratio (TR) of RNA Pol II-Ser 2p at c-MYC and TAF5L bound genes in *Taf5l* KO and wild-type.

(D) The traveling ratio (TR) of RNA Pol II-Ser 2p at c-MYC and TAF6L bound genes in *Taf6l* KO and wild-type.

(E) The traveling ratio (TR) of RNA Pol II-Ser 5p at c-MYC and TAF5L bound genes in *Taf5l* KO and wild-type.

(F) The traveling ratio (TR) of RNA Pol II-Ser 5p at c-MYC and TAF6L bound genes in *Taf6l* KO and wild-type.

Related to Figure 5.

Figure S6

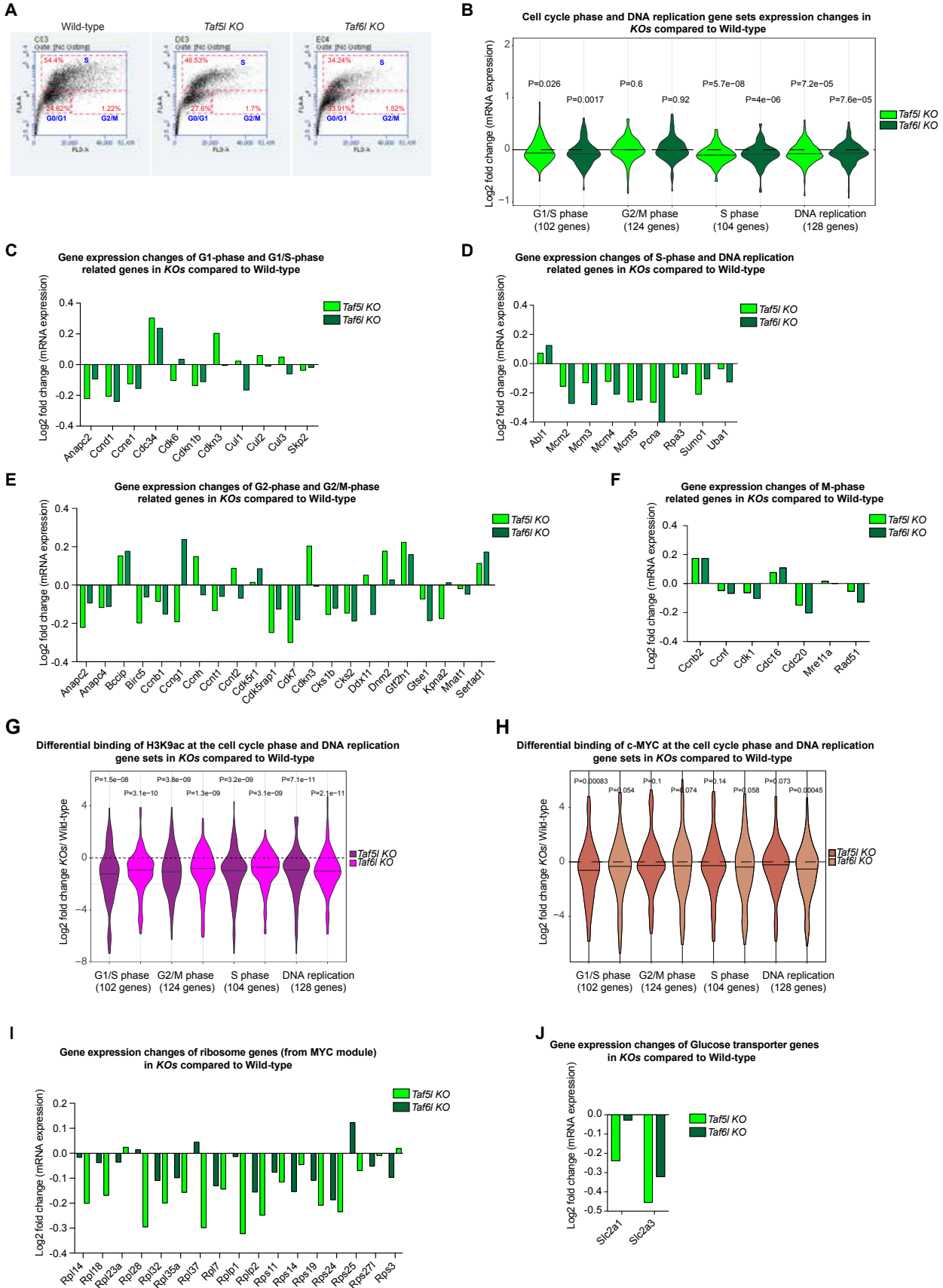


Figure S6. TAF5L/TAF6L maintain self-renewal of mESCs through MYC regulatory module/network

(A) FACS plots of cell cycle profiling from wild-type, *Taf5l* KO and *Taf6l* KO.

(B) Gene expression changes of different phases of the cell cycle and DNA replication gene sets in *Taf5l* and *Taf6l* KOs compared to wild-type.

(C-F) Gene expression changes of several individual genes related to different phases of the cell cycle and DNA replication in *Taf5l* and *Taf6l* KOs compared to wild-type.

(G, H) Differential binding of H3K9ac (G) and c-MYC (H) at the cell cycle phase and DNA replication gene sets in *Taf5l* and *Taf6l* KOs compared to wild-type.

(I) Gene expression changes of ribosome genes of MYC module in *Taf5l* and *Taf6l* KOs compared to wild-type.

(J) mRNA expression levels of glucose transporter genes in *Taf5l* and *Taf6l* KOs compared to wild-type.

Related to Figure 6.

Figure S7

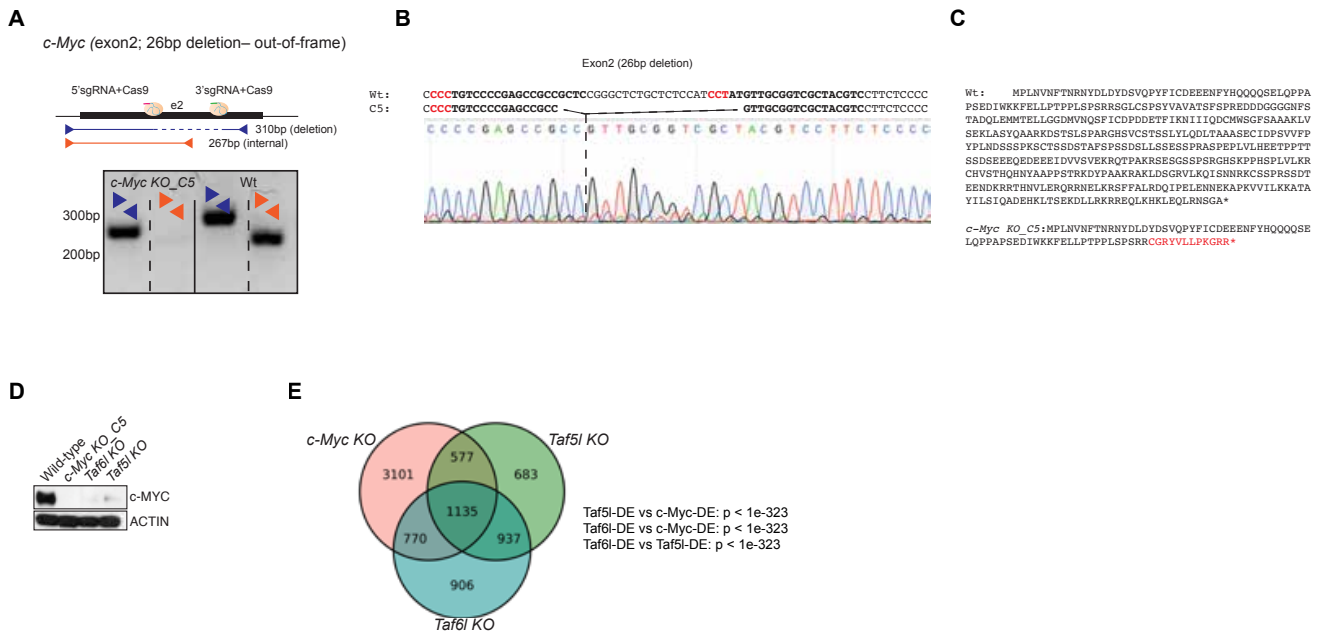


Figure S7. TAF5L/TAF6L and c-MYC work together, as well as independently for gene regulation

(A) Strategy to generate homozygous deletion or *KO* clone of *c-Myc* in mESCs. Paired sgRNAs (5' and 3' sgRNAs) were used to target exon 2 of *c-Myc* that create homozygous deletion/*KO* of *c-Myc*. Two PCRs (deletion PCR and internal PCR) were used to identify biallelic/homozygous deletion.

(B) Sanger sequencing showing a biallelic 26bp deletion at the *c-Myc* coding sequence.

(C) The protein sequence of wild-type c-MYC, and the predicted protein sequence upon 26bp deletion of *c-Myc* gene (*c-Myc KO- clone C5*) are shown. The 26bp deletion created a frameshift mutation that resulted in a premature stop codon.

(D) c-MYC protein levels detected by Western blot in wild-type, *c-Myc KO*, *Taf5l KO* and *Taf6l KO* mESCs.

(E) Venn diagram illustrates overlapping and non-overlapping differentially expressed genes in *c-Myc*, *Taf5l* and *Taf6l KO*s.

Related to Figure 6.